Published in final edited form as:
Osteoarthritis Cartilage. 2009 March ; 17(3): 336–345. doi:10.1016/j.joca.2008.08.001.

TISSUE ENGINEERING WITH MENISCUS CELLS DERIVED FROM SURGICAL DEBRIS

Brendon M. Baker[1,2], **Ashwin S. Nathan**[1,2], **G. Russell Huffman**[1], and **Robert L. Mauck**[1,2]

1 *McKay Orthopaedic Research Laboratory, Department of Orthopaedic Surgery, University of Pennsylvania, Philadelphia, PA 19104*

2 *Department of Bioengineering, University of Pennsylvania, Philadelphia, PA 19104*

Abstract

Objective—Injuries to the avascular regions of the meniscus fail to heal and so are treated by resection of the damaged tissue. This alleviates symptoms but fails to restore normal load transmission in the knee. Tissue engineering functional meniscus constructs for re-implantation may improve tissue repair. While numerous studies have developed scaffolds for meniscus repair, the most appropriate autologous cell source remains to be determined. In this study, we hypothesized that the debris generated from common meniscectomy procedures would possess cells with potential for forming replacement tissue. We also hypothesized that donor age and the disease status would influence the ability of derived cells to generate functional, fibrocartilaginous matrix.

Methods—Meniscus derived cells (MDCs) were isolated from waste tissue of ten human donors (seven partial meniscectomies, three total knee arthroplasties) ranging in age from 18–84 years. MDCs were expanded in monolayer culture through passage two and seeded onto fiber-aligned biodegradable nanofibrous scaffolds and cultured in a chemically-defined media. Mechanical properties, biochemical content, and histological features were evaluated over ten weeks of culture.

Results—Results demonstrated that cells from every donor contributed to increasing biochemical content and mechanical properties of engineered constructs. Significant variability was observed in outcome parameters (cell infiltration, proteoglycan and collagen content, and mechanical properties) amongst donors, but these variations did not correlate with patient age or disease condition. Strong correlations were observed between the amount of collagen deposition within the construct and the tensile properties achieved. In scaffolds seeded with particularly robust cells, construct tensile moduli approached maxima of ~40MPa over the ten week culture period.

Conclusions—This study demonstrates that cells derived from surgical debris are a potent cell source for engineered meniscus constructs. Results further show that robust growth is possible in MDCs from middle-aged and elderly patients, highlighting the potential for therapeutic intervention using autologous cells.

Keywords

Tissue Engineering; Meniscus; Mechanical Properties; Nanofiber; Anisotropy

†Corresponding Author: Robert L. Mauck, Ph.D. Assistant Professor of Orthopaedic Surgery and Bioengineering, McKay Orthopaedic Research Laboratory, Department of Orthopaedic Surgery, University of Pennsylvania, 36th Street and Hamilton Walk, Philadelphia, PA 19104, Phone: (215) 898-3294, Fax: (215) 573-2133, Email: E-mail: lemauck@mail.med.upenn.edu.

Introduction

The meniscus is a fibrocartilaginous tissue vital to knee function[1–5]. Aligned collagen bundles within the meniscus[6] bear tensile hoop stresses that are generated with load transmission across the tibiofemoral joint[7]. These stresses are resisted, with little deformation[8], by the high tensile properties in the circumferential direction, which range from 50–250MPa, depending on age, species, and testing parameters[1, 9–13]. The meniscus is sparsely colonized by a heterogeneous cell population which continually maintains and remodels the extracellular matrix (ECM)[14, 15]. Meniscus cells transition from a fibrochondrocyte-like phenotype in the avascular inner region to a more fibroblastic phenotype in the outer rim, with ECM deposition reflective of this transition (i.e., a mix of type I and type II collagen and aggrecan in the inner zone and type I collagen in the periphery)[14, 16–24].

While the meniscus functions well with a lifetime of use, traumatic or degenerative injuries to the avascular, inner region fail to heal[25]. Disruption of the fibrous architecture impairs load transmission[8, 26, 27] and initiates erosion of the adjacent articular surfaces, or osteoarthritis (OA)[28–31]. Currently, damage to the inner zone of the meniscus is treated by resection via arthroscopic partial meniscectomy, which alleviates symptoms but similarly predisposes patients to OA. Tissue removed in this procedure is deemed surgical waste and is discarded at the time of surgery. Studies following patient outcomes after partial meniscectomy indicate that resection of larger portions of meniscus results in more rapid cartilage erosion[32, 33]. Adverse changes in cartilage (as indicated by radiographic joint space narrowing) are noted within a 5–10 year period post-meniscectomy[30]. This long duration before clinical symptoms arise creates a unique window of opportunity for the application of regenerative strategies to restore meniscus function and avert the onset of OA.

Over the last two decades, a number of tissue engineering strategies have emerged to replace all or part of the meniscus to improve immediate and long-term patient outcomes (reviewed in [34–36]). For example, cell-free hydrogels have been implanted in place of an entire meniscus in rabbit and sheep models[37, 38]. A variety of degradable porous foams have been developed[39, 40], some incorporating anchors for fixation to the tibial plateau[41], or carbon fibers to instill directionality[42]. More recently, efforts have focused on natural materials such as subintestinal submucosa[43, 44] as well as collagen- and tissue- based implants[45–49]. Many of these studies employing *in vivo* animal models reveal that some chondroprotection is afforded by the implant, but that none to date have been able to recapitulate native mechanical properties or completely abrogate cartilage degeneration[50].

To further the field of meniscus repair, we have investigated the use of nanofibrous scaffolds combined with meniscal cells or mesenchymal stem cells for meniscus tissue engineering[51, 52]. This strategy is founded on electrospinning, a scaffold fabrication technique that generates nanometer diameter fibers through an electrostatic process[53, 54]. While numerous biologic and synthetic polymers can be electrospun (see 54 for review), we fabricate nanofibrous scaffolds using poly(ε-caprolactone), a slowly degrading polyester. This polymer was chosen as it maintains its form in a physiologic environment and can thus direct tissue formation over a long period of time (as cells deposit new ECM), as well as deform elastically over physiologic ranges experienced in the meniscus[55]. These fibers can further be arranged into parallel arrays[51, 52, 56, 57], creating an architecturally and mechanically anisotropic micro-pattern conducive to organized tissue growth. In a recent study, we showed that young bovine meniscal cells aligned with and deposited ECM in the predominant fiber direction of these anisotropic scaffolds, and that this matrix deposition improved the construct tensile properties with time in culture[52]. Such constructs, that possess architectural and mechanical features similar to the native tissue, may better restore meniscus mechanics and load transmission *in vivo*, averting the onset of OA after meniscus repair.

To move this technology closer to clinical implementation, this study focused on the potential of human meniscus derived cells (MDCs) isolated from surgical debris from patients undergoing either partial meniscectomy or total knee arthroplasty (TKA). Isolation of cells from native meniscus tissue has a number of advantages; the cells have the appropriate phenotype, would be autologous and so limit immune responses, and requires no secondary surgical site. In this study, we utilized cells derived from ten patients spanning a range of ages (18–84 years old) and disease conditions (traumatic or degenerative meniscus lesions, or OA of the entire joint). It has previously been shown that increases in organism age limits the ability of chondrocytes from articular cartilage to form functional ECM[58, 59]. Further, when age-matched chondrocytes derived for autologous chondrocyte implantation procedures were compared between normal and osteoarthritic donors, cells from diseased tissues showed a markedly lower ability to form collagen-rich ECM[60]. Meniscus cells are related to chondrocytes (particularly for the samples acquired from the inner avascular region of the meniscus), and so we hypothesized that while all surgical specimens would yield viable human cells, their ability to deposit functional fibrocartilaginous ECM and improve scaffold properties would depend on the donor age and/or disease status. To test this hypothesis, MDCs were seeded onto aligned nanofibrous scaffolds, cultured in a chemically defined chondrogenic medium, and biochemical, histological, and mechanical properties were evaluated over a ten week time course.

Materials and Methods

Scaffold Fabrication

For each donor, a separate aligned, nanofibrous mesh was produced via electrospinning[51, 52]. Briefly, a 14.3% w/v solution of poly(ε-caprolactone) (PCL) (80kD, Sigma-Aldrich, St. Louis, MO) was dissolved in a 1:1 solution of tetrahydrofuran and N,N-dimethylformamide (Fisher Chemical, Fairlawn, NJ). The solution was electrospun onto a grounded mandrel (1″ diameter, 8″ length) rotating at a velocity of ~10 meters/sec[51]. For each production run, nanofibers were collected for 8 hours, resulting in a fiber mats with an average thickness of 0.865 ± 0.177mm.

Cell Isolation, Expansion, and Seeding

Meniscus tissue was collected according to an approved IRB protocol from ten adult male and female patients ranging in age from 18 to 84 years (See Table 1). Resected tissue was finely minced and plated on tissue culture polystyrene in basal medium (DMEM containing 1X PSF and 10% FBS). Meniscus-derived cells (MDCs) emerged over a two week period after which the tissue pieces were removed. Adherent colonies were passaged twice to obtain $>20\times10^6$ cells for scaffold seeding.

Mechanically homogeneous strips (5mm wide by 75mm long) were cut in the prevailing fiber direction of electrospun sheets and prepared for cell-seeding[51, 52]. Strips were disinfected in ethanol (100, 70, 50, 30%; 30 minutes per step), rinsed twice in phosphate-buffered saline (PBS), and soaked overnight in a 20μg/ml human fibronectin (Invitrogen, Carlsbad, CA). Prior to seeding, strips were rinsed twice with PBS and segmented into three 25mm long pieces, two of which were seeded with MDCs, leaving one to serve as a paired, unseeded control (USC). For seeding, each scaffold side received a 50μl aliquot containing 250,000 cells followed by one hour of incubation. After the final incubation, seeded constructs were cultured in 4mL of chemically-defined medium (high glucose DMEM with 1X PSF, 0.1μM dexamethasone, 50μg/mL ascorbate 2-phosphate, 40μg/mL L-proline, 100μg/mL sodium pyruvate, 1X ITS+ (6.25μg/ml Insulin, 6.25μg/ml Transferrin, 6.25ng/ml Selenous Acid, 1.25mg/ml Bovine Serum Albumin, and 5.35μg/ml Linoleic Acid) with 10ng/mL TGF-β3) in non-tissue culture

treated 6-well plates[61]. The USCs were incubated at 37°C in PBS changed twice monthly for the study duration.

Mechanical Testing

Uniaxial tensile testing was performed with an Instron 5848 Microtester (Instron, Canton, MA). Prior to testing, five thickness measurements along the length of each sample were taken with a custom LVDT measurement system; five width measurements were acquired with a digital caliper. Samples were clamped in serrated grips and a 0.5N preload applied for 180 seconds to ensure proper seating. After noting gauge length with a digital caliper, samples were preconditioned by cyclic extension to 0.5% of the gauge length 0.1Hz for 10 cycles. Subsequently, samples were extended beyond their yield point at a rate of 0.1% of the gauge length per second. For day 70 samples, extension was carried out until failure occurred. Stiffness was determined from the linear region of the force-elongation curve. Using the cross-sectional area and gauge length, Young's modulus was calculated from the analogous stress-strain curve. Five seeded samples were tested for each of the ten donors at each time point along with their corresponding USCs.

Biochemical Analyses

After mechanical testing, samples were stored at −80°C until determination of biochemical composition. Samples were lyophilized (Freezone 4.5 Freeze Dry System, LabConco, Kansas City, MO) for 24 hours and massed to determine dry weights. Following this, samples were papain digested as in [61] and DNA, sulfated glycosaminoglycan (s-GAG), and collagen content was determined using the Picogreen double-stranded DNA (dsDNA) (Molecular Probes, Eugene, OR), DMMB dye-binding[62], and hydroxyproline[63] assays, respectively. Hydroxyproline content was converted to collagen as in [64], using a factor of 7.14. This conversion is an estimate, and susceptible to bias based on the prevailing collagen type present. Data are reported as a sample's total content or as a percentage of the sample dry weight. Five additional human meniscus samples (donor age 62 ± 6 years, all TKAs) were tested to establish native tissue biochemical content ranges.

Histology

Cytoskeletal organization was examined in MDC monolayers and cell-laden constructs one day post-seeding. Filamentous actin and nuclei were labeled with Alexa Flour 647 phalloidin and Prolong Gold Antifade with DAPI (Invitrogen), respectively, and imaged at 20× on a Nikon T30 inverted fluorescent microscope (Nikon Instruments, Inc., Melville, NY). For analysis of matrix deposition with long-term culture, a 6mm length was cut from each paired, non-tested construct, fixed overnight at 4°C in 4% phosphate-buffered paraformaldehyde, and frozen in Optimal Cutting Temperature compound (Sakura Finetek USA, Inc., Torrance, CA). Cross-sections, 8μm thick (spanning the depth and width of the scaffold) were cut with a Cryostat (Microm HM500, MICROM International GmbH, Waldorf, Germany). Sections were rehydrated and stained with DAPI, Alcian Blue (AB, pH 1.0), or Picrosirius Red (PSR) to visualize cell nuclei, proteoglycans, or collagen, respectively. DAPI stained sections were imaged at 5×. On separate slides, AB and PSR images were acquired at the same magnification on an upright Leica DMLP microscope (Leica Microsystems, Germany).

Statistical Analyses

Analysis of variance (ANOVA) was carried out with SYSTAT (v10.2, Point Richmond, CA). Fisher's LSD post-hoc tests were used to make pair-wise comparisons between donors and time points, with significance set at $p \leq 0.05$. At least 5 samples were analyzed for each donor at each time point. Data are presented as the mean ± standard deviation for each donor. Pearson's correlation analysis was performed with SYSTAT.

Results

Cell Isolation, Expansion, and Scaffold Seeding

Cells were successfully isolated from meniscus tissue from each of the ten donors (Table 1). A total of 20×10^6 passage 2 cells were required from each donor for construct seeding. The time from initial plating to passage 2 confluency with sufficient expansion ($>20\times10^6$ cells) was 53 ± 9.6 days. Cell morphology (Figure 1) during expansion showed an increasing population of fibroblast-like cells. When seeded onto aligned scaffolds, MDCs aligned their long axes and cytoskeleton with the scaffold architecture (Figure 1).

Mechanical Properties of MDC-Laden Constructs

Mechanical properties of cell-seeded and paired acellular scaffolds were assessed via tensile testing. It was noted in preliminary studies that variations in scaffold mechanical properties exist both between different nanofibrous PCL batches, as well as along the length of the collection mandrel. For example, scaffold stiffness on day 14 (before appreciable matrix deposition) from different batches ranged from 2.7 to 6.1N/mm (Table 2). To address the issue, each donor was assigned a specific production run of nanofibrous scaffold, and each MDC-seeded sample was tested along with an unseeded control (USC) excised from the same location along the mandrel. As strips excised in such a manner begin with identical mechanical properties, the effect of cell-seeding and ECM deposition can be more accurately assessed. By normalizing the stiffness of each cell-seeded scaffold to its counterpart USC at each time point, a percentage change (as well as a magnitude change) in stiffness can be determined.

The mechanical response of engineered constructs differed markedly between USC and MDC-seeded constructs over the duration of the study. The force-displacement curve from each of the day 70 Donor 8 samples are shown in Figure 2A, with MDC-laden constructs showing a much higher stiffness and ultimate load. Quantification of these changes amongst all donors revealed that the ultimate load (Figure 2B) and stiffness (Figure 2C) of cell-seeded samples increased for 8/10 donors and 10/10 donors by day 70, respectively ($p<0.001$ vs. USC). Conversely, USC did not decrease over this same time course ($p>0.219$ vs. day 14). The average change in stiffness between day 14 and day 70 was 4.2 ± 2.1N/mm for all donors, with a maximum change of 8.1N/mm for Donor 8 and a minimum change of 1.6N/mm for Donor 6 (Table 2). On a percentage basis, this represents changes of up to 300% in construct stiffness compared to USC over the 70 days (Figure 2C). Cell-seeded constructs from each of the donors also increased in thickness ($p<0.05$ except Donors 4 and 6), resulting in an increasing cross-sectional area (Table 2, $p<0.05$ except donors 4 and 6). While moduli generally increased, the effect of the increase in cross-sectional area occasionally precluded these changes from reaching significance (Table 2). The average change in modulus was 9.1 ± 6.8MPa for all donors, with a maximum change of 21.6MPa for Donor 8 and a minimum change of 0.8MPa for Donor 9.

Biochemical Content of MDC-Laden Constructs

Construct biochemical content was determined for cell-seeded scaffolds with time in culture. Constructs seeded with MDCs from all donors increased in dry weight (Table 3, $p<0.05$ except Donor 2). This increase in mass ranged between 2.5mg (Donor 4) and 6.1mg (Donor 9) and averaged 4.5 ± 1.6mg for all donors. DNA content also increased with time in culture ($p<0.001$) for all donors except for Donor 10 (Table 3). Collagen and s-GAG contents also increased in constructs in a time-dependent manner (Figure 3A, 3B, $p<0.001$). Overall, the total s-GAG and collagen per construct was highly dependent on time in culture ($p<0.001$) and donor ($p<0.001$). We normalized these results to the dry weight (DW) of the construct (Figure 3C, 3D) to enable comparisons to the native tissue. For collagen, native tissue values averaged 50 ± 18% DW, and ranged from 24 to 72% DW (Figure 3C, grey region, note break in scale). S-

GAG content of native tissue averaged 0.6 ± 0.3% DW, and ranged from 0.3 to 1.1% DW (Figure 3D, grey region). The most robust deposition of collagen (~18% DW, Donor 5) was lower than the lowest native tissue level, while the largest amount of GAG (~3.3% DW, Donor 7) was above native levels.

Structure-Function Correlations of MDC-Seeded Constructs

Correlation analysis was carried out to determine the structure-function relationships within developing constructs, and the relationship between donor age and capacity to generate increasing mechanical properties (Figure 4A–C). Strong correlations were found between the change in stiffness of the construct with the total collagen content (Figure 4A, R^2=0.81 value, $p<0.001$). Weaker (but significant) correlations were also observed for change in stiffness with total s-GAG content (Figure 4B, R^2=0.46, $p<0.001$). While there were significant differences in total DNA content between donors, no correlation was observed between this measure and mechanical performance (data not shown). Finally, correlating the change in stiffness with age showed a weak correlation toward increasing properties with donor age (Figure 4C, R^2=0.47, $p<0.05$).

Histological Analysis

Cellular infiltration and distribution of ECM was evaluated through histological staining of construct cross-sections. DAPI-staining showed the progressive infiltration of cells into the scaffold with culture time. Cells from different donors infiltrated to a greater or lesser degree as shown in the best-case (Figure 5A, Donor 8) and worst-case (Figure 5B, Donor 6) images of day 70 samples. Similarly, collagen and s-GAG deposition varied amongst donors and appeared to correlate with the best performing (Figure 5C, 5E) and worst performing (Figure 5D, 5F) constructs on day 70.

Discussion

In this study, we assessed the ability of human meniscal derived cells (MDCs) to modulate the properties of fiber-aligned biodegradable electrospun nanofibrous scaffolds. This scaffolding system serves as a 3D micro-pattern for directing cell orientation and neo-tissue formation by replicating the structural and mechanical anisotropy of the native tissue. Human MDCs were isolated from surgical waste from ten human donors ranging in age from 18–84 and with differing disease status (acute versus degenerative meniscus tears or progression of knee osteoarthritis necessitating total joint replacement). MDCs were successfully isolated from each donor tissue, expanded in culture through passage 2, seeded onto scaffolds, and cultured in a chemically-defined, pro-fibrocartilaginous medium formulation for ten weeks. When seeded with MDCs, construct tensile properties, biochemical content, and histological features improved with time. Amongst the ten donors, variations were observed in the magnitude of these quantitative and qualitative outcome measures, but each donor MDC population yielded positive maturation of the engineered construct. Those donors whose MDCs responded most vigorously generated well infiltrated constructs containing ~25% of the collagen content of the native tissue with tensile moduli of ~40MPa. These findings indicate that native human MDCs derived from surgical debris are a potent cell source for the fabrication of mechanically functional engineered meniscus constructs.

We began this work with the hypothesis that MDCs derived from older individuals would harbor less capacity to generate functional properties *in vitro*. This idea was predicated on work demonstrating that in chondrocytes, a related cell type, collagen production decreases with age[58, 59], and that disease states such as osteoarthritis further reduce the matrix forming capacity[60]. In this study, MDCs were derived from the inner third of the meniscus (small avascular tears), the inner two-thirds of the meniscus (large tears or degenerate regions), or

from the entirety of the meniscus (meniscus removal with TKA). These MDCs represented a range of donor ages, spanning 18–84 years. MDCs from the inner zone of the meniscus are considered chondrocyte-like, displaying phenotypic similarities including a round cell shape and cartilage gene expression and matrix deposition[23, 65]. Thus, these cells were expected to display age-dependent declines in ECM deposition capacity. However, counter our hypothesis, the age of donor MDCs showed no negative correlation with the properties of the engineered construct. In fact, in this study, change in stiffness and donor age showed a weak positive correlation. This finding is perhaps due the fact that all donors were at or beyond skeletal maturity, while the most marked changes in cell biosynthetic activities occur at early ages. Interestingly, constructs with the most proteoglycan deposition, which one would expect for MDCs derived from the inner zone, actually came from Donor 9, who underwent a TKA and contributed cells from the entire meniscus. Obviously, these findings are drawn from a small set of donors, but analysis of this set reveals few strong indicators of robust growth based on standard parameters such as age and zonal source of donor cells.

In this study we focused on MDCs isolated from meniscectomy debris as a cell source for engineering replacement meniscus tissue. We focus on this overlooked cell source for a number of reasons outlined above (potential for autologuous therapies, no immune response, proper cell phenotype), and not on the more commonly used mesenchymal stem cell (MSC). MSCs can undergo a fibrocartilaginous differentiation on nanofibrous scaffolds, as evidenced by increases in aggrecan and type II collagen expression and deposition[66], and we have demonstrated similar growth and maturation patterns when using MSCs compared to MDCs in a juvenile bovine model system[52]. However, MSC isolation necessitates a second surgical site not associated with primary meniscus repair. Furthermore, we have recently shown that all regions of the meniscus contain multipotential cells[67], suggesting that endogenous cell populations may contribute to repair processes. The finding that all constructs improved in mechanical properties from ten donors, points to the potential of MDCs as a cell source for meniscus tissue engineering. With surgery, the defect that is generated to alleviate acute symptoms may be accurately characterized. As the time between meniscus injury and the onset of OA is relatively long (5–10 years), a fully conforming construct may be fabricated and matured *ex vivo* to effect autologous repair.

In vitro culture of meniscus implants offers a range of benefits, most importantly the ability to optimize neo-tissue growth. In this study, we used a chemically defined medium containing TGF-β3 to promote fibrocartilaginous ECM deposition. In our previous studies with MDCs in both pellet format and when seeded onto nanofibrous scaffolds, this medium increased proteoglycan and collagen deposition[52, 67]. For a small subset of four donors, expression (assessed by real time PCR) of aggrecan and type I collagen was constant or increased over the culture duration, while type II collagen expression increased markedly, perhaps reflecting the reversal of dedifferentiation events that had occurred as result of monolayer expansion (data not shown). For the repair of defects in the inner avascular meniscus zone (the most common site of injury in middle-aged patients), engineered constructs would ideally match the biochemical composition of the native tissue. This zone contains the largest level of proteoglycan, and a mixture of type I and type II collagen[21]. For MDCs from all donors, GAG levels matched or were superior to native tissue. Correlations between measured GAG content and tensile properties showed only a weak correlation. Conversely, collagen content of constructs formed from all donors increased substantially, and reached a maximum of 18% of the dry weight of the native tissue, though a range is observed in samples derived from differing states of meniscal degeneration. Correlation analysis showed a very strong association between collagen deposition in constructs and the tensile properties. This suggests that maximizing the collagen content of constructs may further improve their tensile properties.

While the results of this study are promising, there are several limitations that should be addressed. First, significant variations were observed in the properties achieved amongst the ten donors. Age does not appear to be the prevailing indicator, and so other predictors of growth potential must be developed to identify suitable donors, such as short term screening in pellet cultures prior to scaffold seeding. Furthermore, while some constructs approached moduli of 40 MPa within ten weeks, further enhancement of this and other mechanical properties towards native tissue values is a priority. Another potential limiting factor is the persistence of the polymer fibers, which may impede complete cellular infiltration. While the volume fraction of polymer in these scaffolds is in the range of 10–20%[51], small pores may slow matrix filling. Inclusion of faster degrading polymer elements, such as PLGA or PGA[55], or biologic fiber components such as collagen[68], into the fibrous network may speed this infiltration process. Alternatively, infiltration may be enhanced by creating a mixture of fiber sizes[69], utilizing salt leaching approaches to create large pores/lamellae[70], or as in our recent approach, evacuating sacrificial fibers to enhance porosity while maintaining overall structural anisotropy[71].

As a final note, we created constructs as rectangular strips to facilitate tensile testing, without considering the wedge-shaped anatomic form of the meniscus. For clinical application, engineering and fabrication technologies must be developed to enable reproduction of the anatomic form, and integration with native tissue must be achieved[72]. To this end, we have recently demonstrated that MDC-seeded multi-lamellar constructs form mechanically viable interfaces when held in apposition with one another[73] and with the native tissue[74], and that the constructs hold suture[75] allowing fixation within a meniscus defect. Regardless of these advances, complete integration will be a significant challenge[76], and strategies that engage the outer vascular periphery[77] maybe be required to enable *in vivo* success. Long-term *in vivo* studies will address this question in detail, and explore the ability of these novel constructs to preserve articular cartilage and avert the onset of OA after partial meniscectomy.

Acknowledgements

This work was supported via pilot funding from the Penn Center for Musculoskeletal Disorders (AR050950), an Orthopaedic Medicine Research Grant from the Aircast Foundation (F0206R), and a Medical Research Grant from the NFL Charities. Additional support was provided by a Department of Education GAANN Fellowship and a National Science Foundation Graduate Research Fellowship (BMB). The authors also gratefully acknowledge Dr. Neil P. Sheth and Dr. Charles L. Nelson for their assistance in tissue acquisition.

References

1. Fithian DC, Kelly MA, Mow VC. Material properties and structure-function relationships in the menisci. Clin Orthop 1990:19–31. [PubMed: 2406069]
2. Messner K, Gao J. The menisci of the knee joint. Anatomical and functional characteristics, and a rationale for clinical treatment J Anat 1998;193 (Pt 2):161–78.
3. Kelly, MA.; Fithian, DC.; Chern, KY.; Mow, VC. Structure and function of the meniscus: basic and clinical applications. In: Mow, VC.; Ratcliffe, A.; Woo, SL-Y., editors. Biomechanics of Diarthrodial Joints. Vol. 1. New York: Springer-Verlag; 1990. p. 191-211.
4. Walker PS, Erkman MJ. The role of the menisci in force transmission across the knee. Clin Orthop Relat Res 1975:184–92. [PubMed: 1173360]
5. Ahmed, AM. The load-bearing role of the knee meniscus. Knee meniscus: basic and clinical foundations. Mow, VC.; Arnoczky, SP.; Jackson, DW., editors. New York: Raven Press, Ltd.; 1992. p. 59-73.
6. Petersen W, Tillmann B. Collagenous fibril texture of the human knee joint menisci. Anat Embryol (Berl) 1998;197:317–24. [PubMed: 9565324]
7. Shrive NG, O'Connor JJ, Goodfellow JW. Load-bearing in the knee joint. Clin Orthop 1978:279–87. [PubMed: 657636]

8. Jones RS, Keene GC, Learmonth DJ, Bickerstaff D, Nawana NS, Costi JJ, et al. Direct measurement of hoop strains in the intact and torn human medial meniscus. Clin Biomech (Bristol, Avon) 1996;11:295–300.
9. Mow, VC.; Ratcliffe, A.; Chern, KY.; Kelly, MA. Structure and function relationships of the menisci of the knee. In: Mow, VC.; Arnoczky, SP.; Jackson, DW., editors. Knee meniscus: basic and clinical foundations. New York: Raven Press, Ltd.; 1992. p. 37-57.
10. Bullough PG, Munuera L, Murphy J, Weinstein AM. The strength of the menisci of the knee as it relates to their fine structure. J Bone Joint Surg Br 1970;52:564–7. [PubMed: 5468789]
11. Tissakht M, Ahmed AM. Tensile stress-strain characteristics of the human meniscal material. J Biomech 1995;28:411–22. [PubMed: 7738050]
12. Proctor CS, Schmidt MB, Whipple RR, Kelly MA, Mow VC. Material properties of the normal medial bovine meniscus. J Orthop Res 1989;7:771–82. [PubMed: 2677284]
13. Sweigart MA, Zhu CF, Burt DM, DeHoll PD, Agrawal CM, Clanton TO, et al. Intraspecies and interspecies comparison of the compressive properties of the medial meniscus. Ann Biomed Eng 2004;32:1569–79. [PubMed: 15636116]
14. Arnoczky SP. Building a meniscus. Biologic considerations. Clin Orthop Relat Res 1999:S244–53. [PubMed: 10546650]
15. Benjamin M, Ralphs JR. Biology of fibrocartilage cells. Int Rev Cytol 2004;233:1–45. [PubMed: 15037361]
16. Verdonk PC, Forsyth RG, Wang J, Almqvist KF, Verdonk R, Veys EM, et al. Characterisation of human knee meniscus cell phenotype. Osteoarthritis Cartilage 2005;13:548–60. [PubMed: 15979007]
17. Cheung HS. Distribution of type I, II, III and V in the pepsin solubilized collagens in bovine menisci. Connect Tissue Res 1987;16:343–56. [PubMed: 3132349]
18. Kambic HE, McDevitt CA. Spatial organization of types I and II collagen in the canine meniscus. J Orthop Res 2005;23:142–9. [PubMed: 15607886]
19. Spindler KP, Miller RR, Andrish JT, McDevitt CA. Comparison of collagen synthesis in the peripheral and central region of the canine meniscus. Clin Orthop Relat Res 1994:256–63. [PubMed: 8194243]
20. McDevitt CA, Webber RJ. The ultrastructure and biochemistry of meniscal cartilage. Clin Orthop Relat Res 1990:8–18. [PubMed: 2406077]
21. Adams, ME.; Hukins, DWL. The extracellular matrix of the meniscus. Knee meniscus: basic and clinical foundations. Mow, VC.; Arnoczky, SP.; Jackson, DW., editors. New York: Raven Press, Ltd.; 1992. p. 15-28.
22. Hellio Le Graverand MP, Ou Y, Schield-Yee T, Barclay L, Hart D, Natsume T, et al. The cells of the rabbit meniscus: their arrangement, interrelationship, morphological variations and cytoarchitecture. J Anat 2001;198:525–35. [PubMed: 11430692]
23. Nakata K, Shino K, Hamada M, Mae T, Miyama T, Shinjo H, et al. Human meniscus cell: characterization of the primary culture and use for tissue engineering. Clin Orthop Relat Res 2001:S208–18. [PubMed: 11603705]
24. Valiyaveettil M, Mort JS, McDevitt CA. The concentration, gene expression, and spatial distribution of aggrecan in canine articular cartilage, meniscus, and anterior and posterior cruciate ligaments: a new molecular distinction between hyaline cartilage and fibrocartilage in the knee joint. Connect Tissue Res 2005;46:83–91. [PubMed: 16019418]
25. Newman AP, Anderson DR, Daniels AU, Dales MC. Mechanics of the healed meniscus in a canine model. Am J Sports Med 1989;17:164–75. [PubMed: 2667375]
26. Levy IM, Torzilli PA, Gould JD, Warren RF. The effect of lateral meniscectomy on motion of the knee. J Bone Joint Surg Am 1989;71:401–6. [PubMed: 2925713]
27. Krause WR, Pope MH, Johnson RJ, Wilder DG. Mechanical changes in the knee after meniscectomy. J Bone Joint Surg Am 1976;58:599–604. [PubMed: 946970]
28. Rath E, Richmond JC. The menisci: basic science and advances in treatment. Br J Sports Med 2000;34:252–7. [PubMed: 10953895]
29. Roos H, Adalberth T, Dahlberg L, Lohmander LS. Osteoarthritis of the knee after injury to the anterior cruciate ligament or meniscus: the influence of time and age. Osteoarthritis Cartilage 1995;3:261–7. [PubMed: 8689461]

30. Roos H, Lauren M, Adalberth T, Roos EM, Jonsson K, Lohmander LS. Knee osteoarthritis after meniscectomy: prevalence of radiographic changes after twenty-one years, compared with matched controls. Arthritis Rheum 1998;41:687–93. [PubMed: 9550478]

31. Elliott DM, Guilak F, Vail TP, Wang JY, Setton LA. Tensile properties of articular cartilage are altered by meniscectomy in a canine model of osteoarthritis. J Orthop Res 1999;17:503–8. [PubMed: 10459755]

32. Cox JS, Nye CE, Schaefer WW, Woodstein IJ. The degenerative effects of partial and total resection of the medial meniscus in dogs' knees. Clin Orthop Relat Res 1975:178–83. [PubMed: 1173359]

33. Andersson-Molina H, Karlsson H, Rockborn P. Arthroscopic partial and total meniscectomy: A long-term follow-up study with matched controls. Arthroscopy 2002;18:183–9. [PubMed: 11830813]

34. Setton LA, Guilak F, Hsu EW, Vail TP. Biomechanical factors in tissue engineered meniscal repair. Clin Orthop 1999:S254–72. [PubMed: 10546651]

35. Sweigart MA, Athanasiou KA. Toward tissue engineering of the knee meniscus. Tissue Eng 2001;7:111–29. [PubMed: 11304448]

36. Buma P, Ramrattan NN, van Tienen TG, Veth RP. Tissue engineering of the meniscus. Biomaterials 2004;25:1523–32. [PubMed: 14697855]

37. Kobayashi M, Chang YS, Oka M. A two year in vivo study of polyvinyl alcohol-hydrogel (PVA-H) artificial meniscus. Biomaterials 2005;26:3243–8. [PubMed: 15603819]

38. Kelly BT, Robertson W, Potter HG, Deng XH, Turner AS, Lyman S, et al. Hydrogel meniscal replacement in the sheep knee - Preliminary evaluation of chondroprotective effects. American Journal of Sports Medicine 2007;35:43–52. [PubMed: 16957008]

39. van Tienen TG, Heijkants RG, Buma P, de Groot JH, Pennings AJ, Veth RP. Tissue ingrowth and degradation of two biodegradable porous polymers with different porosities and pore sizes. Biomaterials 2002;23:1731–8. [PubMed: 11950043]

40. Heijkants RG, van Calck RV, De Groot JH, Pennings AJ, Schouten AJ, van Tienen TG, et al. Design, synthesis and properties of a degradable polyurethane scaffold for meniscus regeneration. J Mater Sci Mater Med 2004;15:423–7. [PubMed: 15332611]

41. Chiari C, Koller U, Dorotka R, Eder C, Plasenzotti R, Lang S, et al. A tissue engineering approach to meniscus regeneration in a sheep model. Osteoarthritis Cartilage 2006;14:1056–65. [PubMed: 16731009]

42. Veth RP, Jansen HW, Leenslag JW, Pennings AJ, Hartel RM, Nielsen HK. Experimental meniscal lesions reconstructed with a carbon fiber-polyurethane-poly(L-lactide) graft. Clin Orthop Relat Res 1986:286–93. [PubMed: 3754190]

43. Cook JL, Fox DB, Malaviya P, Tomlinson JL, Farr J, Kuroki K, et al. Evaluation of small intestinal submucosa grafts for meniscal regeneration in a clinically relevant posterior meniscectomy model in dogs. J Knee Surg 2006;19:159–67. [PubMed: 16893153]

44. Cook JL, Fox DB, Malaviya P, Tomlinson JL, Kuroki K, Cook CR, et al. Long-term Outcome for Large Meniscal Defects Treated With Small Intestinal Submucosa in a Dog Model. Am J Sports Med 2006;34:32–42. [PubMed: 16157845]

45. Stone, KR.; Rodkey, WG.; Webber, RJ.; McKinney, LA.; Steadman, JR. Development of a prosthetic meniscal replacement. Knee meniscus: basic and clinical foundations. Mow, VC.; Arnoczky, SP.; Jackson, DW., editors. New York: Raven Press, Ltd.; 1992. p. 165-73.

46. Martinek V, Ueblacker P, Braun K, Nitschke S, Mannhardt R, Specht K, et al. Second generation of meniscus transplantation: in-vivo study with tissue engineered meniscus replacement. Arch Orthop Trauma Surg 2005:1–7.

47. Izuta Y, Ochi M, Adachi N, Deie M, Yamasaki T, Shinomiya R. Meniscal repair using bone marrow-derived mesenchymal stem cells: experimental study using green fluorescent protein transgenic rats. Knee 2005;12:217–23. [PubMed: 15911296]

48. Rodkey WG, Steadman JR, Li ST. A clinical study of collagen meniscus implants to restore the injured meniscus. Clin Orthop Relat Res 1999:S281–92. [PubMed: 10546653]

49. Zaffagnini S, Giordano G, Vascellari A, Bruni D, Neri MP, Iacono F, et al. Arthroscopic collagen meniscus implant results at 6 to 8 years follow up. Knee Surg Sports Traumatol Arthrosc 2007;15:175–83. [PubMed: 16845545]

50. Tienen TG, Heijkants RG, de Groot JH, Pennings AJ, Schouten AJ, Veth RP, et al. Replacement of the knee meniscus by a porous polymer implant: a study in dogs. Am J Sports Med 2006;34:64–71. [PubMed: 16260465]
51. Li WJ, Mauck RL, Cooper JA, Yuan X, Tuan RS. Engineering controllable anisotropy in electrospun biodegradable nanofibrous scaffolds for musculoskeletal tissue engineering. J Biomech 2007;40:1686–93. [PubMed: 17056048]
52. Baker BM, Mauck RL. The effect of nanofiber alignment on the maturation of engineered meniscus constructs. Biomaterials 2007;28:1967–77. [PubMed: 17250888]
53. Li D, Xia YN. Electrospinning of nanofibers: Reinventing the wheel? Advanced Materials 2004;16:1151–70.
54. Li WJ, Mauck RL, Tuan RS. Electrospun nanofibrous scaffolds: production, characterization, and applications for tissue engineering and drug delivery. J Biomed Nanotech 2005;1:259–75.
55. Li WJ, Cooper JA Jr, Mauck RL, Tuan RS. Fabrication and characterization of six electrospun poly (alpha-hydroxy ester)-based fibrous scaffolds for tissue engineering applications. Acta Biomater 2006;2:377–85. [PubMed: 16765878]
56. Courtney T, Sacks MS, Stankus J, Guan J, Wagner WR. Design and analysis of tissue engineering scaffolds that mimic soft tissue mechanical anisotropy. Biomaterials 2006;27:3631–8. [PubMed: 16545867]
57. Ayres C, Bowlin GL, Henderson SC, Taylor L, Shultz J, Alexander J, et al. Modulation of anisotropy in electrospun tissue-engineering scaffolds: Analysis of fiber alignment by the fast Fourier transform. Biomaterials 2006;27:5524–34. [PubMed: 16859744]
58. Tran-Khanh N, Hoemann CD, McKee MD, Henderson JE, Buschmann MD. Aged bovine chondrocytes display a diminished capacity to produce a collagen-rich, mechanically functional cartilage extracellular matrix. J Orthop Res 2005;23:1354–62. [PubMed: 16048738]
59. Barbero A, Grogan S, Schafer D, Heberer M, Mainil-Varlet P, Martin I. Age related changes in human articular chondrocyte yield, proliferation and post-expansion chondrogenic capacity. Osteoarthritis Cartilage 2004;12:476–84. [PubMed: 15135144]
60. Tallheden T, Bengtsson C, Brantsing C, Sjogren-Jansson E, Carlsson L, Peterson L, et al. Proliferation and differentiation potential of chondrocytes from osteoarthritic patients. Arthritis Res Ther 2005;7:R560–8. [PubMed: 15899043]
61. Mauck RL, Yuan X, Tuan RS. Chondrogenic differentiation and functional maturation of bovine mesenchymal stem cells in long-term agarose culture. Osteoarthritis Cartilage 2006;14:179–89. [PubMed: 16257243]
62. Farndale RW, Buttle DJ, Barrett AJ. Improved quantitation and discrimination of sulphated glycosaminoglycans by use of dimethylmethylene blue. Biochim Biophys Acta 1986;883:173–7. [PubMed: 3091074]
63. Stegemann H, Stalder K. Determination of hydroxyproline. Clin Chim Acta 1967;18:267–73. [PubMed: 4864804]
64. Neuman RE, Logan MA. The determination of hydroxyproline. J Biol Chem 1950;184:299–306. [PubMed: 15421999]
65. Upton ML, Chen J, Setton LA. Region-specific constitutive gene expression in the adult porcine meniscus. J Orthop Res 2006;24:1562–70. [PubMed: 16732608]
66. Li WJ, Tuli R, Huang X, Laquerriere P, Tuan RS. Multilineage differentiation of human mesenchymal stem cells in a three-dimensional nanofibrous scaffold. Biomaterials 2005;26:5158–66. [PubMed: 15792543]
67. Mauck RL, Martinez-Diaz GJ, Yuan X, Tuan RS. Regional variation in meniscal fibrochondrocyte multi-lineage differentiation potential: implications for meniscal repair. Anatomical Record 2007;290:48–58.
68. Telemeco TA, Ayres C, Bowlin GL, Wnek GE, Boland ED, Cohen N, et al. Regulation of cellular infiltration into tissue engineering scaffolds composed of submicron diameter fibrils produced by electrospinning. Acta Biomater 2005;1:377–85. [PubMed: 16701819]
69. Pham QP, Sharma U, Mikos AG. Electrospun Poly(epsilon-caprolactone) Microfiber and Multilayer Nanofiber/Microfiber Scaffolds: Characterization of Scaffolds and Measurement of Cellular Infiltration. Biomacromolecules 2006;7:2796–805. [PubMed: 17025355]

70. Nam J, Huang Y, Agarwal S, Lannutti J. Improved cellular infiltration in electrospun fiber via engineered porosity. Tissue Eng 2007;13:2249–57. [PubMed: 17536926]

71. Baker BM, Gee AO, Metter RB, Nathan AS, Marklein RA, Burdick JA, et al. The potential to improve cell infiltration in composite fiber-aligned electrospun scaffolds by the selective removal of sacrificial fibers. Biomaterials 2008;29:2348–58. [PubMed: 18313138]

72. Sheth NP, Baker BM, Huffman GR, Mauck RL. Emerging Strategies for Meniscus Repair. University of Pennsylvania Orthopaedic Journal 2006;18:59–72.

73. Baker BM, O'Connell GD, Sen S, Nathan AS, Elliott DM, Mauck RL. Multi-lamellar and multi-axial maturation of cell-seeded fiber-reinforced tissue engineered constructs. Proc BIO2007 Summer Bioengineering Conference 2007:176434.

74. Sheth NP, Baker BM, Nathan AS, Mauck RL. Biologic Integration of Fiber-Aligned Nanofibrous Scaffolds with Native Meniscus. Trans Orthop Res Soc 2007;32:711.

75. Sheth NP, Li WJ, Tuan RS, Elliott DM, Huffman GR, Mauck RL. Fixation of anisotropic biodegradable nanofibrous poly-caprolactone scaffolds to bovine meniscus with non-absorbable suture: A strategy for meniscal repair. Trans Orthop Res Soc 2006;31:800.

76. Hennerbichler A, Moutos FT, Hennerbichler D, Weinberg JB, Guilak F. Repair Response of the Inner and Outer Regions of the Porcine Meniscus In Vitro. Am J Sports Med. 2007

77. Arnoczky, SP. Gross and vascular anatomy of the meniscus and its role in meniscal healing, regeneration, and remodeling. In: Mow, VC.; Arnoczky, SP.; Jackson, DW., editors. Knee meniscus: basic and clinical foundations. New York: Raven Press, Ltd.; 1992. p. 1-14.

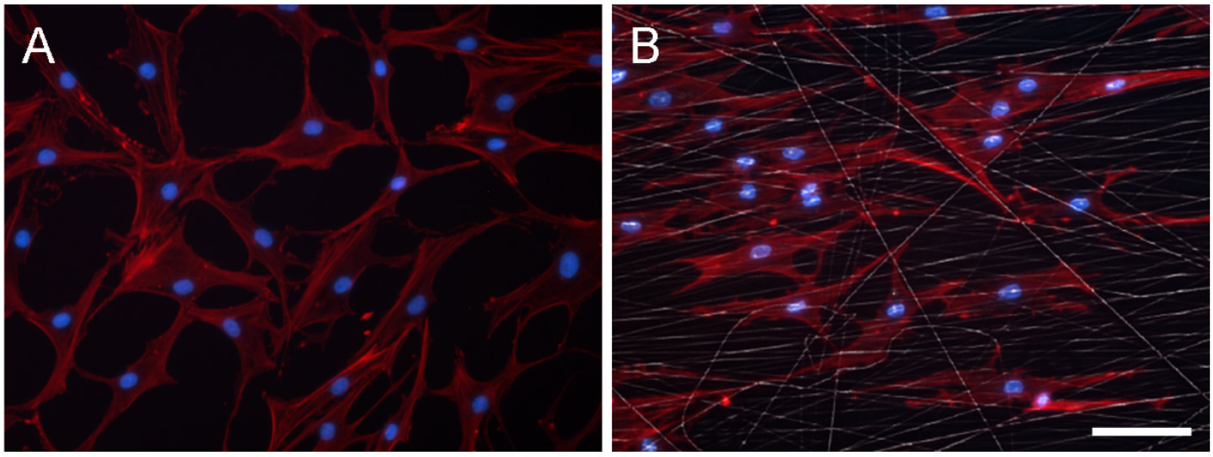

Figure 1. Morphological appearance of passage 2 human MDCs in monolayer and on fiber-aligned nanofibrous scaffolds

(A) Passage 2 MDCs in monolayer on tissue culture polystyrene demonstrate a fibroblast-like morphology. (B) Passage 2 MDC-seeded constructs cultured for one day reveal MDCs elongating in and aligning with the predominant fiber direction of the scaffold. Red: F-actin, white: fibers, blue: nuclei. Scale bar: 50μm.

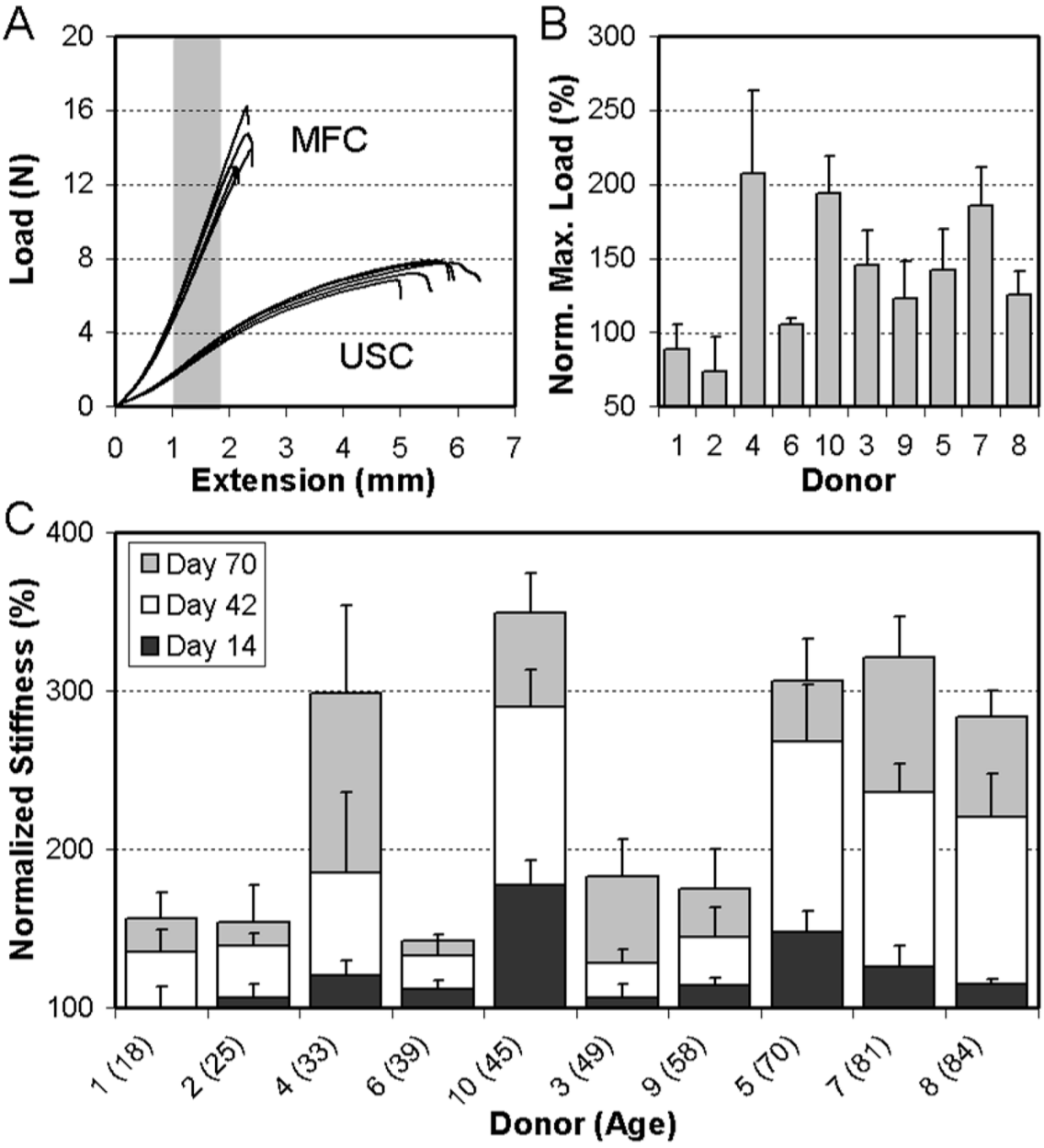

Figure 2. MDC-seeded scaffolds increase in mechanical properties with time in culture in a fibro-cartilaginous medium

(A) Force-elongation plots of five scaffolds either seeded (MDC) or maintained as unseeded controls (USC) on day 70 for Donor 8. (B) Maximum load of seeded scaffolds normalized to that of paired USC scaffolds on day 70 for all ten donors. Donor # is indicated on the x-axis. Data represent the mean and standard deviation of 5 samples per donor. (C) Normalized stiffness (indicating percentage change) of MDC-seeded scaffolds from each donor compared to their paired USC scaffolds at each time point. Donor # (and age) is indicated on the x-axis.

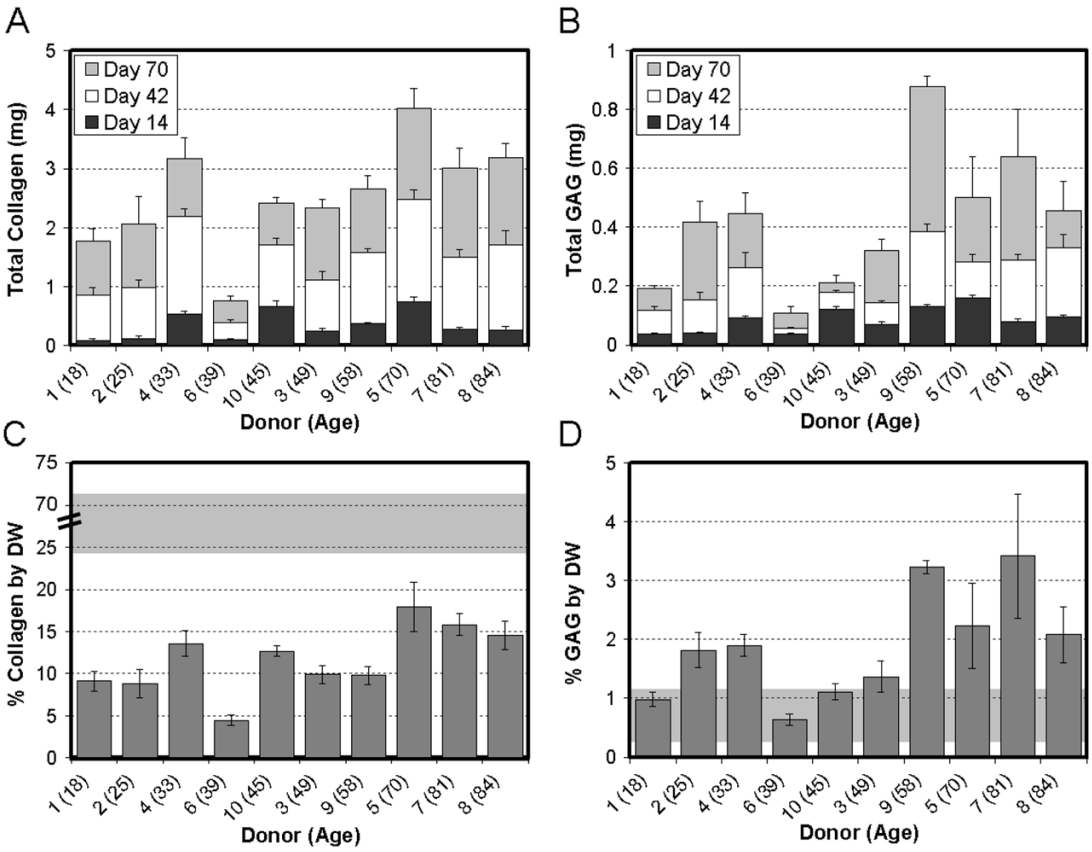

Figure 3. Donor-to-donor variation in time-dependent changes in biochemical composition of MDC-seeded engineered meniscus constructs

(A) Total collagen and (B) total s-GAG accumulation in engineered constructs with time in culture for each donor. Donor # (and age) is indicated on the x-axis. Data represent the mean and standard deviation of 5 samples per donor per time point. (C) Percent dry weight (% DW) collagen and (D) % DW s-GAG for samples from each of the ten donors on day 70. Gray background in (C) and (D) indicates range of collagen and s-GAG found in 5 native tissue samples. Note the interrupted scale in (C) the % collagen by DW plot. USC constructs processed similarly showed no appreciable background content of s-GAG or collagen.

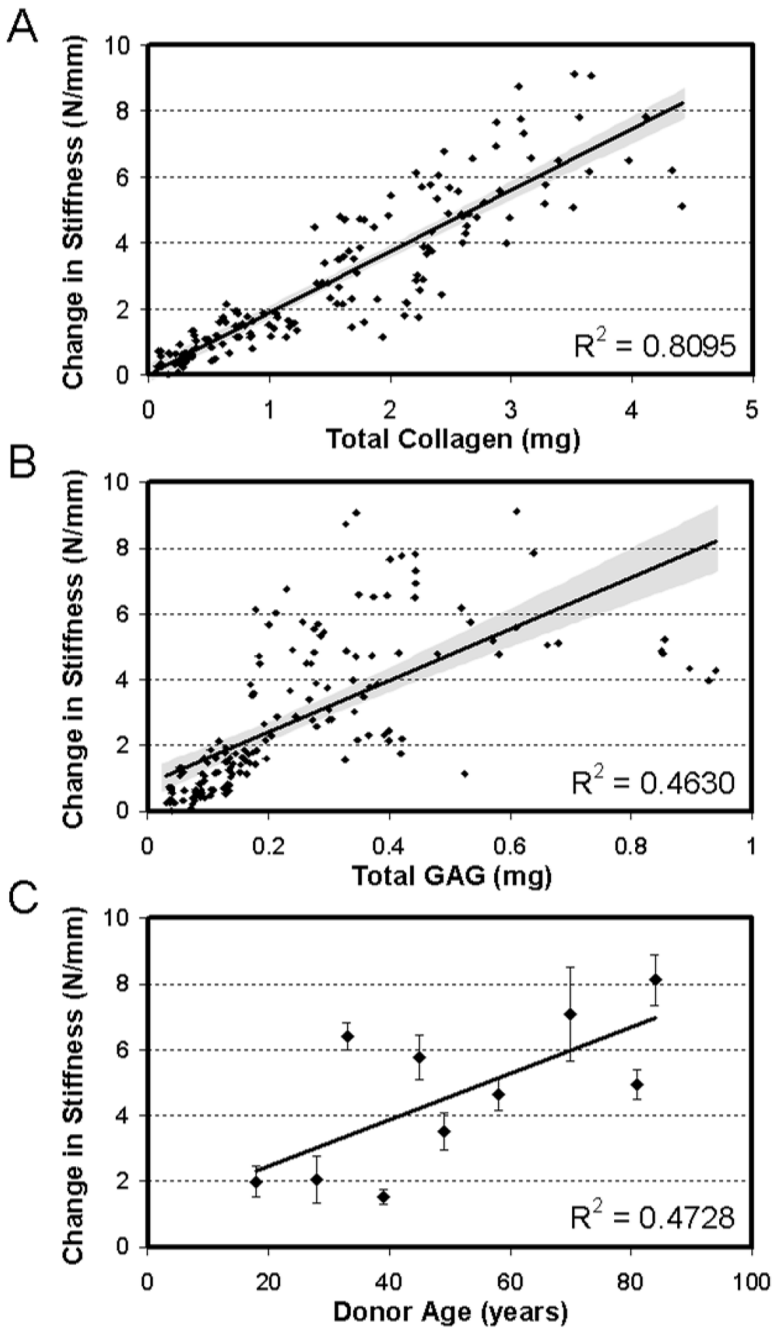

Figure 4. Structure-function-composition correlations for MDC-seeded constructs with time in culture

(A) Total collagen content in constructs correlates well with change in stiffness for all donors at all time points (days 14, 42, and 70). (B) Total GAG content correlates poorly with change in stiffness for all donors at all time points (days 14, 42, and 70). (C) Donor age showed a weak correlation with change in stiffness of constructs on day 70.

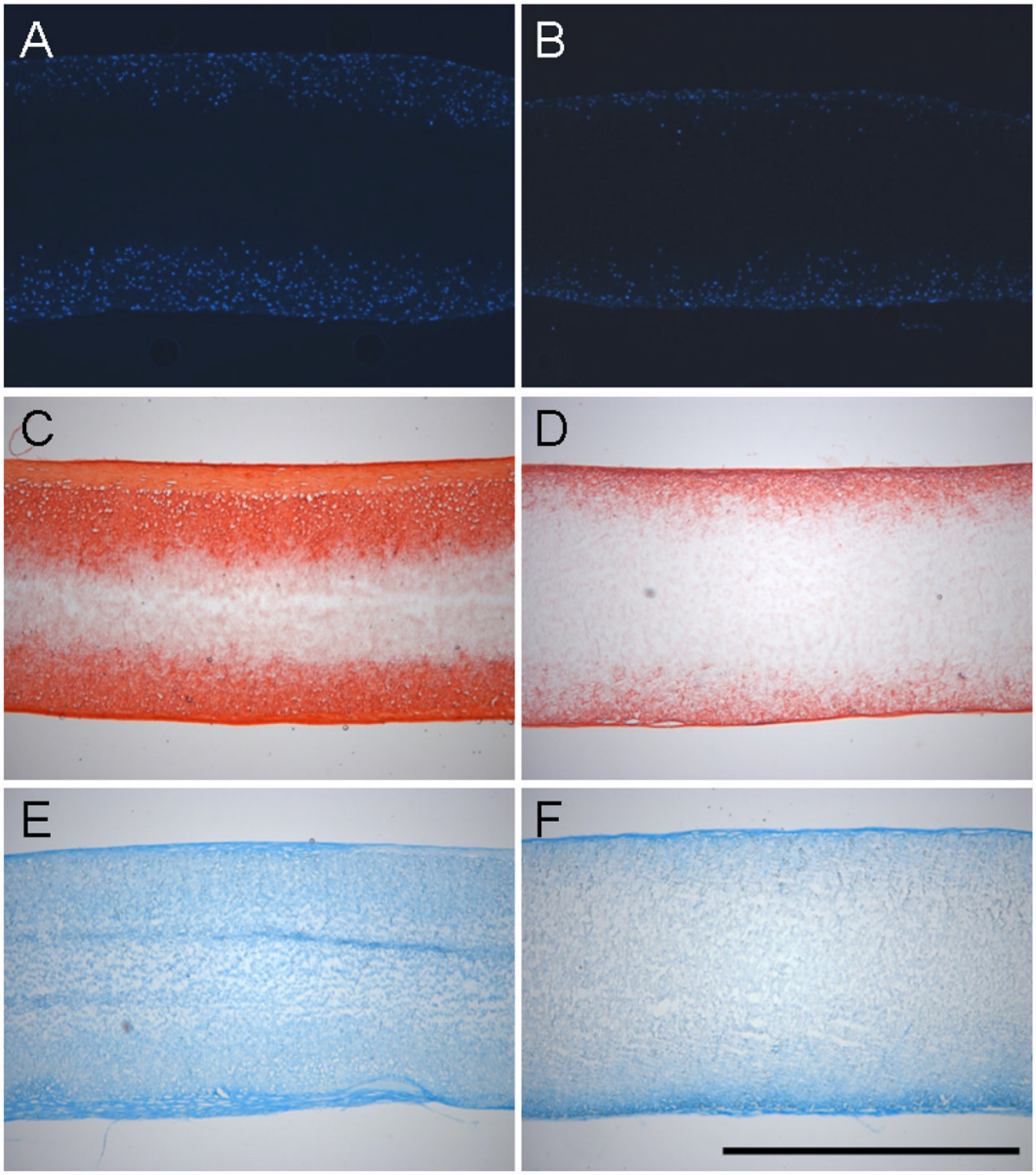

Figure 5. Histological analysis of constructs from best-case (Donor 8, A,C,E) and worst-case (Donor 6, B,D,F) samples on day 70

DAPI staining of cell nuclei demonstrate infiltration into the outer two-thirds of constructs under best-case conditions (A), and limited infiltration at the periphery under worst-case conditions (B). Similar findings are observed for collagen (C,D) and proteoglycan (E,F) deposition as indicated by Picrosirius Red and Alcian Blue staining, respectively. Scale Bar: 1mm.

Table 1

Characteristics of Human Donor Tissue: Age, Gender, Tear Type, and Anatomic Location

Surgical debris from a total of ten donors ranging in age from 18-84 years was used in this study. Tissue was derived from seven donors who underwent partial meniscectomy and three who underwent total knee replacement.

Donor	Age	Sex	Tear Type	Side	Location
1	18	Male	Bucket handle	Medial	Inner 2/3
2	25	Male	Incomplete discoid	Lateral	Inner 1/3
3	49	Male	Radial	Medial	Inner 2/3
4	33	Male	Bucket handle	Medial	Inner 1/3
5	70	Male	TKA	Medial	Total
6	39	Male	Radial	Medial	Inner 1/3
7	81	Male	Radial-horizontal	Medial	Inner 2/3
8	84	Female	TKA	N/A	Total
9	58	Male	TKA	Lateral	Total
10	45	Female	Horizontal	Lateral	Inner 2/3

Table 2

Structural and Mechanical Properties of Engineered Meniscus Constructs

Cross-sectional area (CSA, mm^2), Stiffness (N/mm), Modulus (MPa), and Maximum Stress (MPa) achieved on day 70 are provided for constructs generated from each of the ten donors. Values indicate the mean (top number in bold) and standard deviation (bottom number) of five samples tested for each measure and donor at each time point. For each parameter, the highest magnitude of change is denoted with an (H), and lowest level of change is denoted with an (L). Average change in each parameter between days 14 and 70 for all donors is provided at the bottom of each column. An asterisk indicates significant difference with $p<0.05$ in a given parameter compared to its day 14 value.

		CSA (mm^2)		Stiffness (N/mm)		Modulus (MPa)		Max Stress (Mpa)
Time in Culture		Day 14	Day 70	Day 14	Day 70	Day 14	Day 70	Day 70
Donor (Age)	**1 (18)**	**4.6** 1.1	**5.4 +** 0.6	**3.7** 0.3	**5.6** 0.3	**16.1** 3.2	**20.2** 2.4	**4.6** 1.1
	2 (25)	**5.0** 0.5	**6.3** 0.6	**4.2** 0.3	**5.9** 0.5	**15.3** 1.3	**17.2 +** 1.0	**5.7** 0.4
	4 (33)	**5.5** 0.9	**5.5 +,L** 1.1	**4.6** 0.5	**9.9** 0.9	**15.5** 2.0	**32.5** 5.2	**3.1** 0.6
	6 (39)	**4.0** 0.5	**4.7 +** 0.4	**3.5** 0.4	**5.1L** 0.5	**15.4** 1.2	**19.2** 0.6	**2.8** 0.4
	10 (45)	**4.0** 0.4	**4.7** 0.4	**3.8** 0.5	**8.1** 0.8	**16.9** 0.4	**30.2** 1.4	**2.0** 0.2
	3 (49)	**5.0** 0.5	**6.1** 0.7	**4.1** 0.6	**7.9** 0.4	**15.0** 0.9	**23.1** 1.8	**3.2** 0.5
	9 (58)	**4.5** 0.9	**7.6 H** 0.5	**6.1** 1.9	**11.2** 1.0	**24.8** 4.1	**25.6 +,L** 1.1	**5.6** 1.5
	5 (70)	**4.2** 0.4	**5.9** 0.5	**4.9** 0.3	**10.5** 1.7	**21.2** 1.9	**31.5** 3.4	**3.1** 0.5
	7 (81)	**3.6** 0.3	**5.2** 0.3	**2.7** 0.1	**7.2** 0.6	**13.9** 0.6	**23.9** 1.4	**2.3** 0.3
	8 (84)	**4.3** 0.4	**5.5** 0.4	**4.2** 0.7	**12.5 H** 1.0	**17.6** 1.4	**39.2 H** 1.6	**4.8** 0.6
	Average Δ	**1.2** 0.8		**4.2** 2.1		**9.1** 6.8		**3.7** 1.3

Table 3

Biochemical Composition of Engineered Meniscus Constructs

Dry mass (mg), total DNA content (μg), total sGAG content (μg), and total collagen content (μg) achieved on day 70 are provided for constructs generated from each of the ten donors. Values indicate the mean (top number in bold) and standard deviation (bottom number) of five samples tested for each measure and donor at each time point. For each parameter, the highest magnitude of change is denoted with an (H), and lowest level of change is denoted with an (L). Average change in each parameter between days 14 and 70 for all donors is provided at the bottom of each column. For this table, all comparisons between days 14 and 70 were significantly different with $p<0.05$ except when noted (+).

		Dry Mass (mg)		Total DNA (μg)		Total GAG (μg)		Total Collagen (μg)	
Time in Culture		Day 14	Day 70	Day 14	Day 70	Day 14	Day 70	Day 14	Day 70
Donor (Age)	1 (18)	**15.6** 1.4	**19.6** 1.3	**4.2** 0.5	**9.7** 1.2	**36.7** 5.4	**190.7** 11.6	**89.5** 28.4	**1778.6** 204.1
	2 (25)	**20.7** 0.9	**23.0 +,L** 1.2	**4.8** 0.8	**10.9 H** 1.9	**39.9** 3.0	**418.4** 70.7	**117.1** 49.5	**2065.8** 461.1
	4 (33)	**21.1** 3.8	**23.6** 3.6	**7.7** 0.5	**9.7** 0.8	**93.1** 7.0	**447.8** 70.3	**541.9** 45.5	**3175.9** 350.3
	6 (39)	**13.9** 1.8	**17.0** 2.0	**3.2** 0.4	**5.1** 0.4	**36.4** 3.1	**109.4 L** 21.2	**98.8** 14.0	**755.0 L** 89.0
	10 (45)	**15.3** 0.8	**19.0** 0.5	**8.1** 0.7	**8.4 +,L** 0.6	**122.0** 8.0	**212.8** 24.3	**665.3** 97.1	**2414.0** 101.2
	3 (49)	**17.9** 3.1	**23.7** 2.5	**7.0** 0.9	**10.1** 0.5	**70.6** 8.0	**320.2** 40.6	**255.3** 41.4	**2336.5** 135.6
	9 (58)	**20.1** 4.0	**27.2 H** 1.7	**11.0** 0.7	**13.6** 0.8	**132.1** 4.7	**877.1 H** 34.6	**375.4** 18.1	**2656.3** 230.3
	5 (70)	**16.9** 1.3	**22.7** 2.0	**12.8** 0.7	**15.2** 0.8	**160.3** 8.8	**500.3** 137.9	**746.6** 82.5	**4013.6 H** 346.4
	7 (81)	**14.1** 1.2	**19.0** 1.0	**8.3** 0.4	**10.0** 0.7	**80.8** 6.8	**641.0** 158.4	**279.0** 30.5	**3006.3** 339.3
	8 (84)	**16.3** 1.2	**22.0** 1.7	**7.4** 0.4	**12.3** 0.7	**93.9** 8.9	**455.2** 99.3	**267.1** 6.8	**3185.7** 248.0
	Average Δ	**4.5** 1.6		**3.0** 1.9		**330.7** 208.2		**2195.2** 749.3	